- 9 -
TRANSDUCER ARRAYS

INTERACTION EFFECTS IN MULTIPLE TRANSDUCER SYSTEMS

We often use more than one transducer in a system. When these transducers occupy different frequency ranges, then their interaction is one of a crossover, which we have already covered. This chapter is concerned with the effects of using more than one transducer in the same frequency range.

There are a great many ways that we can array transducers, but there are two primary parameters that influence their interaction, the translation of the individual elements and the rotation of these elements. The simplest case is when we have point sources, for then there is only translation to consider. So we will start with a discussion of a flat arrays of point sources.

9.1   Simple Point Source Arrays[1]

We have already studied the fundamental concepts for simple arrays when we talked about the Fourier Transform relationships for sound radiation in Chap. 4. We noted that the sound field of an array of extended sources is simply the product of the Directivity Function (*DF*) of the point source array and the *DF* of the individual sources (where the sources are all identical). Since we have already studied the *DF* for arbitrarily flat sources we will have a more complete picture by looking at the point source array problem

First, we will consider an array of point sources along a line – a line array. We will consider the *DF* for an arbitrary linear array of point sources. It is easy to show that the *DF* is

$$DF(\theta) = \frac{\sin\left(kd\sin\theta\right)}{\sin\left(kb\sin\theta\right)} \tag{9.1.1}$$

2d = the length of the array
2b = the spacing of the points

---

1. See Beranek, *Acoustics*

An example of a polar map for a line array of 1.2 m height with a spacing of .3 m between points (i.e. 5 points) is shown in Fig. 9-1. We saw nearly identical results to these when we studied piston sources. It can be shown that increasing *d*, the length of the array, translates the null lines horizontally to the left (towards lower frequencies) and decreasing *b,* the spacing between the points and hence the number of points, increases the density of the null lines in the vertical (angular) direction. We can think of this map, if normalized, as a plot *of kb* versus *kd*.

Extending our discussion to two dimensions is an easy matter since the solution will be the same polar map shown above along each coordinate direction. It will actually be the same in any direction in the plane of the sources, although scaled differently. The total solution is the product of the two individual coordinate solutions.

The point source example is particularly simple but it clearly demonstrates one of the key aspects of arrays – translation of sources causes severe interactions between the them. We noted this situation when we talked about crossovers and we are seeing it again in dealing with arrays.

It should be apparent that this translation effect can be used to increase the directivity of a small source, which does not have a substantial directivity by itself. Another factor, one which is not obvious, is that the acoustic center of an array is its geometric center, whether or not there is actually a source there. For example, the acoustic center of two sources is directly in the middle of them. In this way, it is possible to get crossovers which do not have a moving acoustic center with fre-
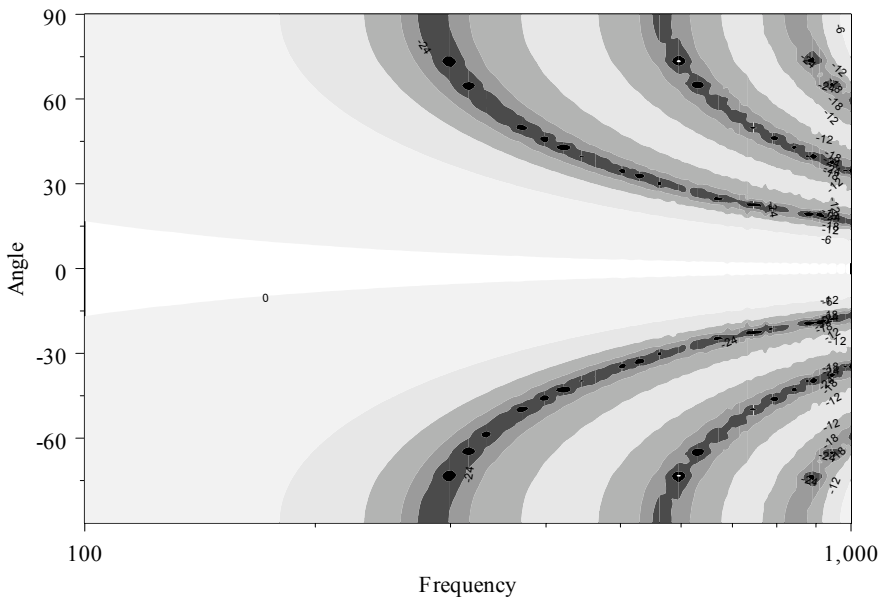

Figure 9-1 - Polar map for a line array of sources

quency. A much lower spatial aberration problem results than what was noted in Chap. 4. Two woofers with a tweeter in the center is an example of this configuration. Although the usual configuration has a single tweeter in the center, a more constant power response would be obtained by using two tweeters spatially separated but with a common acoustic center to the two woofers. This would give a narrower polar pattern in the vertical direction at high frequencies than the use of a single tweeter. Two standard two way loudspeakers can be placed one on top of the other, with the tweeters together, to achieve this design in an amazingly simple manner. We have often used this technique.

We could go on and look at circular arrays and we would find that they would best be studied by using the Hankel Transform, with which we are already familiar. Not being axi-symmetric, however (due to the discrete nature of the points), the solutions would involve Hankel Transforms in higher order modes[2]. We did not look at this modification of the Hankel Transform, but it is a straightforward and logical extension of what we have already seen. We will not develop this technique any further here. Finally, we should note that in the circular case we would have to use the circular convolution integral to get the directivity of a circular array of real sources. While doable, this is not trivial.

We will now move on and look at the effect of rotation on directivity.

9.2   Spherical Arrays

Consider the problem of two sources placed in a sphere, but facing in different directions. This is a close approximation to the design of a loudspeaker cluster as often used in large venues, where numerous drivers are hung together in a complex array to cover a wider area than can be achieved with one transducer alone.

First, consider the directivity map of a flared waveguide in a sphere with intended $60° (\pm 30°)$ coverage. The calculations are performed using the same procedure that we developed in Section 3.1.5. The only difference is that here, the velocity distribution is based on the results for a flared waveguide as we discussed shown in Chap. 6.

The new A_n values are determined from

$$A_n = \left(n + \tfrac{1}{2}\right) \int\limits_{0}^{\frac{\pi}{2b}} V(\theta)\, P_n(\cos\theta)\sin\theta\, d\theta \qquad (9.2.2)$$

where

$$V(\theta) = 1 - \cos\left[b\left(\theta + \frac{\pi}{2b}\right)\right]^6 \qquad (9.2.3)$$

b = a parameter which sets the angular polar response

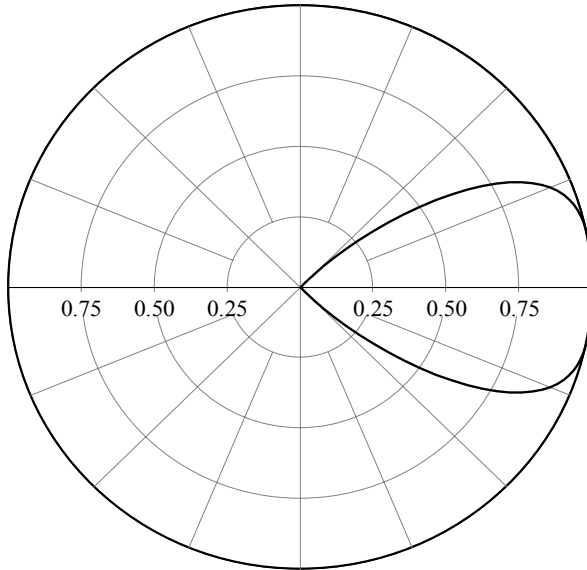2. See Churchill, *Operational Calculus*

Figure 9-2 -   The velocity distribution on the sphere (in cross section)

In our example let $b = 1.8$ which gives the velocity distribution shown in Fig. 9-2. This form for $V(\theta)$ is a convenient way to specify a rapid falloff of velocity with angle in a parametric manner. This velocity distribution can be seen to be about constant – spherically – up to about 20° and to fall off to about 70% of the central value at 30° and to zero at 45°. This is a reasonable assumption for a 60° coverage waveguide which has a flare at its outer edge.

The polar map results are shown in Fig. 9-3 for this single waveguide system. The highest level has been deliberately left transparent to see the underlying grid. The transparent areas in the corners have levels below -40dB. A typical polar map for a coverage angle of 60° can be seen along with the classical midrange narrowing, which is relatively mild in this design.

By using the principle of superposition, we can place a second device on this same sphere and by simply rotating and summing two devices, we can simulate two waveguide mounted in a cluster. This technique ignores the mutual coupling between the two waveguides, but in these frequency ranges this effect is negligible. Fig. 9-4 shows the results of this calculation.

It is readily apparent, and perhaps a bit surprising (perhaps not) that there is virtually no interaction between the two sources. They simply add up to create a polar pattern which is nearly twice the original. Note that even the midrange narrowing effect has been reduced, which is a very pleasing result.

Fig. 9-5 shows a slice of the polar map at 1 kHz (a traditional polar plot). This figure shows two devices which have coincident acoustic centers, angled at 0°,15°
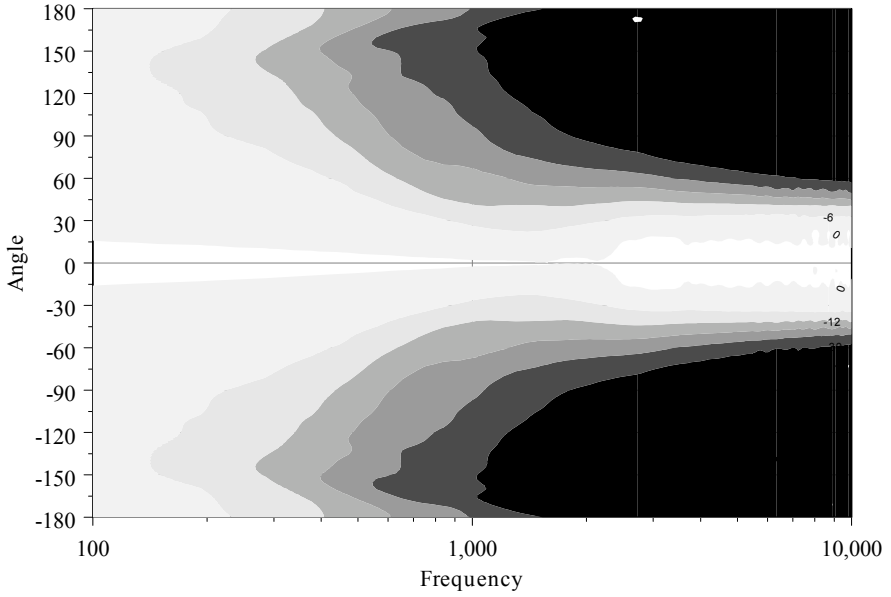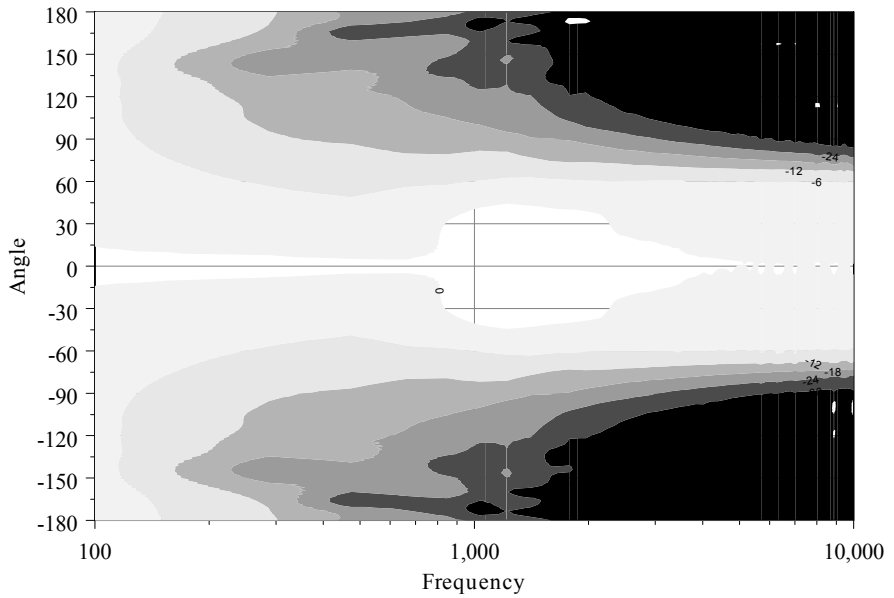
Figure 9-3 - The polar map for a single waveguide sphere

Figure 9-4 - Polar map for two splayed waveguides

0   -6 -12 -18 -24 -30 -36   -36 -30 -24 -18 -12 -6   0
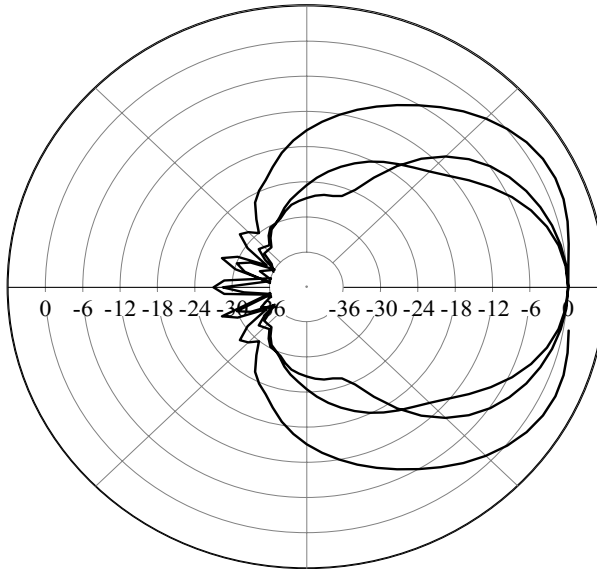
Figure 9-5 - Polar response for two waveguides splayed at 0°, 30° and 60°

and 30° from each other. Note that the polar pattern widens in a predictable manner as the angle between the devices increases. There are no complex interactions.

9.3   Displaced Spherical Arrays

The obvious question now is what happens when the two spherical arrays or spherically divergent wavefronts do not have coincident acoustic centers? This is an easily calculation to make as long as we are willing to accept some inaccuracies. By multiplying the polar calculations by a complex number, which represents the phase delay to the field points due to the displacement of the acoustic centers, we can easily represent the above situation. The problem is that the sphere, in order to be a single solid, would have to become elongated. As long as the translation of the acoustic centers is less than the radius of the sphere, then this issue is not a real concern. Its effect would be limited to those angles beyond 90°, which we are not particularly interested in. The forward pattern would hardly be affected by these errors.

Each spherical source is modified as

$$p(total) = e^{ikr_0 \sin\theta} p_1 + e^{-ikr_0 \sin\theta} p_2 \qquad (9.3.4)$$

r_0 = the displacement of the acoustic centers from the origin

Note that with the above definition, the distance from source to source is $2r_0$.

The polar map for two sources translated by .25 m from the centerline is shown in Fig. 9-6. We can see that the interactions in this case take place primarily
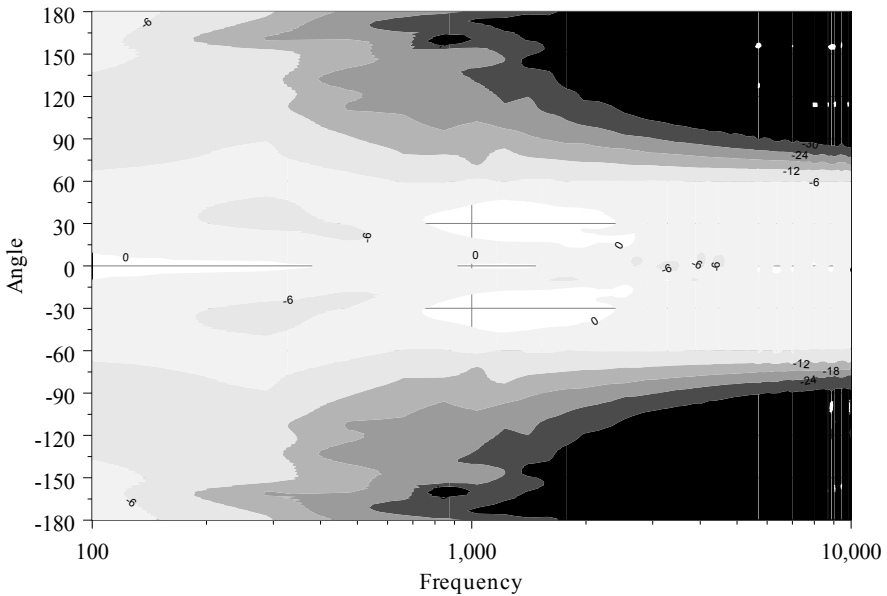

Figure 9-6 - The polar map for two translated and rotated waveguides

at lower frequencies where there is significant overlap of the two sources energies. At the higher frequencies, there is not as much energy outside of the main beam and the interaction diminishes. There are some severe holes near and on the central axis at frequencies around 4 kHz.

In order to better show what is happening, consider Fig. 9-7 This is a polar plot at 1.2 kHz for three translational distances of 0 m, .125 m and .25 m. We can see that the basic polar coverage remains, but the interference ripples increase with increasing translation. It is translation that causes interference, not the use of multiple devices.

The results of this section indicate an important theorem in array design:

> *Devices will simply add, with no interference effects, so long as their acoustic centers are at a common point. Phase interactions and interference results only when the acoustic centers are not coincident, i.e. when the acoustic centers are translated in space.*

Recalling the comments that we made about diffraction horns in Sec. 6.7 on page 161, we can see that lobing will usually occur because of the two acoustic centers, there will always be a translation of one of them. We can array diffraction horns only in one direction as defined by the geometry if we want to avoid lobing problems.
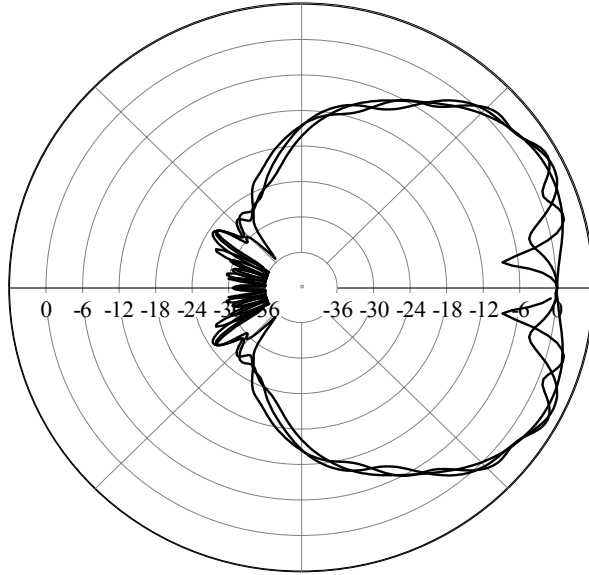
Figure 9-7 - Polar response for three translations of two splayed waveguides

9.4   Line Arrays in Cylindrical Coordinates

By using the results of Sec. 3.6 on page 58, we know that the far field pressure response of a cylindrical source is given by

$$p(R,\theta,\varphi) = -i\sqrt{2}\rho c V_0 \frac{e^{-ikR}}{kR\cos\varphi} \sum_m A_m e^{-im\pi/2} \cos(m\theta) \; \frac{F(k\sin\varphi)}{H_m'\left(ka\sin\varphi\right)} \qquad (9.4.5)$$

where

$$F(k_z) = \frac{1}{2\pi} \int_{-\infty}^{\infty} f(z) e^{-ik_z z} \, dz \qquad (9.4.6)$$

We can see that in the vertical plane, all one has to be concerned with is the Fourier Transform of the vertical velocity distribution – an identical result to that for the line of point sources.

Consider the convolution of a string of point sources of dimension b in the vertical direction separated by a spacing g. The length of the array d we then be $(n\text{-}1)g$ where n is the number of sources. The vertical polar response will be the product of two functions – let's call them DF_p for the point sources and DF_s for the extended sources. We already know these two functions (see Eq. (9.1.1))

$$DF_p(\varphi) = \frac{\sin\big((n-1)\,kg\sin\varphi\big)}{\sin(kg\sin\varphi)} \tag{9.4.7}$$

and

$$DF_s(\varphi) = \frac{\sin(kb\sin\varphi)}{kb\sin\varphi} \tag{9.4.8}$$

and the product is

$$DF(\varphi) = \frac{\sin\big((n-1)\,kg\sin\varphi)\big)}{\sin(kg\sin\varphi)}\,\frac{\sin(kb\sin\varphi)}{kb\sin\varphi} \tag{9.4.9}$$

We can rewrite this equation, with $x = kg\sin\varphi$, as

$$F(x,n,b_g) = \frac{\sin\big((n-1)x\big)}{n\sin(x)}\,\frac{\sin\big(b_g x\big)}{b_g x} \tag{9.4.10}$$

$b_g = b/g < 1.0$ *the ratio of source height to source spacing*

where we have divided by n to normalize the results. With this form for the directivity we can investigate how the vertical pressure response is affected by the percentage of the spacing is taken up by the source. For instance, a value of $b_g = 1$ means that the source is the same height as the spacing and $b_g = .1$ means that the source is only $1/10^{th}$ the vertical size of the spacing.

Fig. 9-8 shows a plot of the directivity function F as a function of $kg\sin\varphi$ and b/g for four sources. Noteworthy in this figure is that the vertical main beam width ($kg\sin\phi \approx 0$) is virtually independent of the individual source height. This can be seen as the vertical lines at the extreme left side of this map, which represents the axial response, i.e. $\varphi = 0$. The only effect that the source size has is on the lobes is at higher frequencies or larger angular values. These can be seen as the arcs along constant values of $kg\sin\varphi \cdot (b/g)$. For $b_g > .7$, there is virtually no practical change in the vertical polar pattern with changing values of b_g.

The next figure (Fig. 9-9) shows the same calculations but with eight individual sources in the array. Little has actually changed in this example other than the lobes continue to be suppressed as we add sources and the directivity becomes even more centrally focussed.

Lastly, we have shown in Fig. 9-10 the calculations for one (bottom) and two (top) elements. The single element map is shown for demonstration only. It really has no meaning other than to show the map for a single source directivity pattern. What is interesting is that we can see this pattern in all the maps, but it gets more and more obscured as the number of sources goes up. Even two sources in the array are enough to obscure the directivity of a single source for all except the highest frequencies or smallest spacing (the upper right-hand corner). The implication is that as soon as there are more than a single source, the array dimensions dominate the situation.
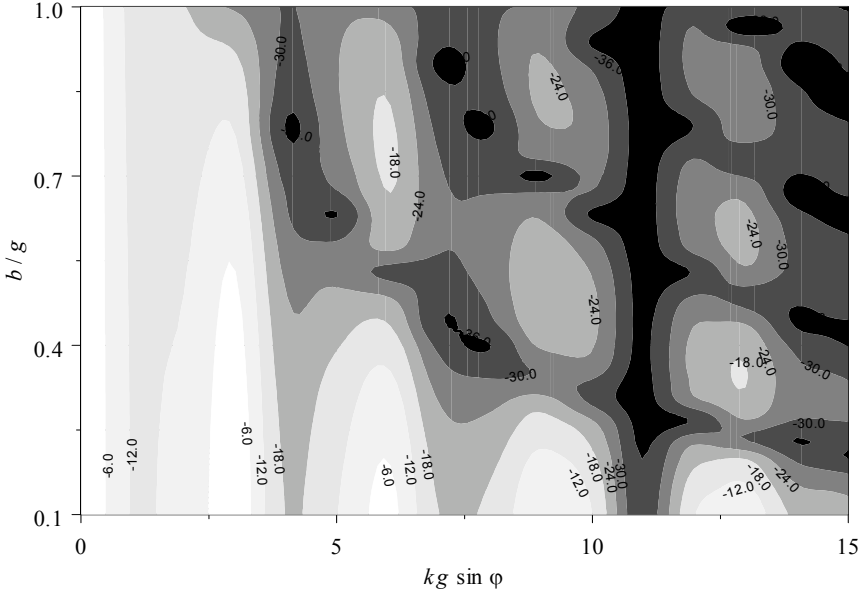
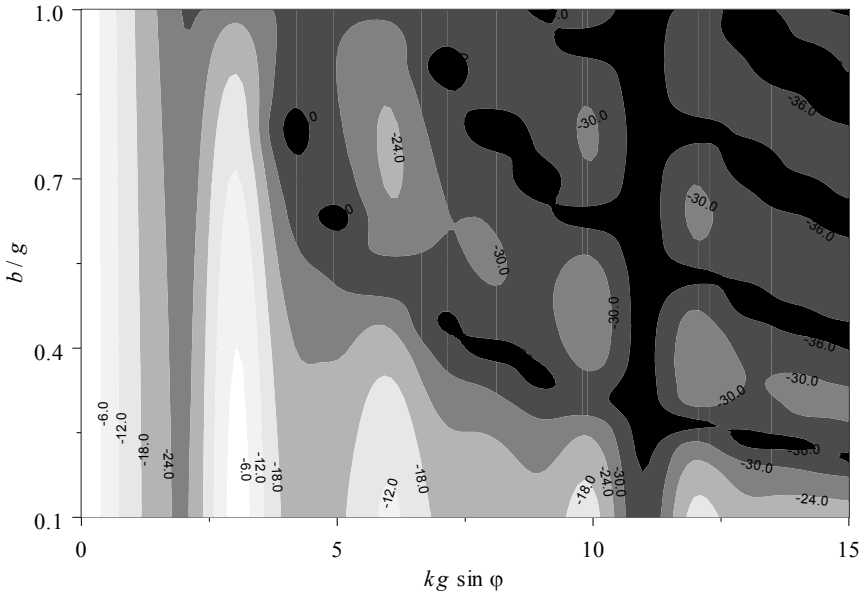*Figure 9-8 - Directivity function for a cylindrical array with 4 elements*

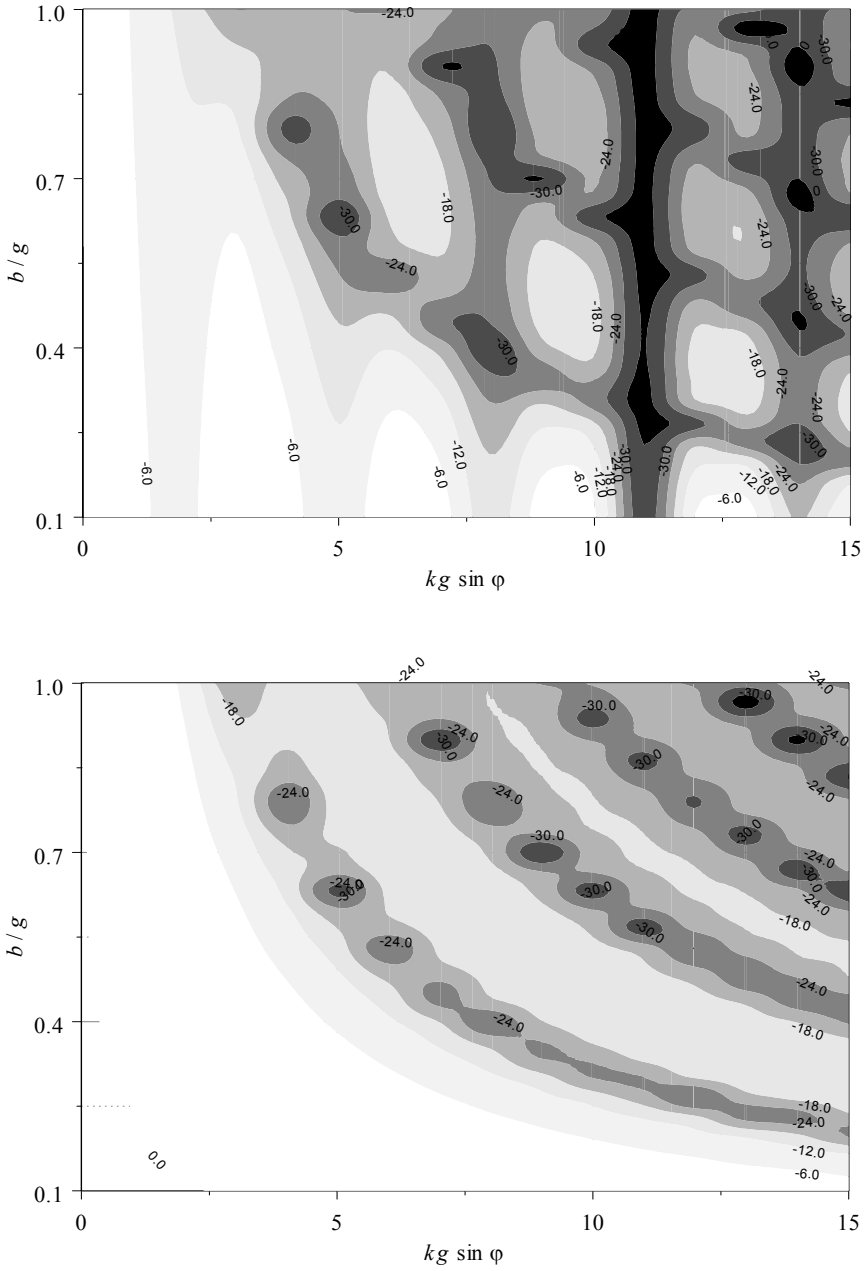*Figure 9-9 - Directivity function for a cylindrical array with 8 elements*

Figure 9-10 - Directivity function for a cylindrical array with 2 (top) and 1 element(s)

We have now seen that arrays offer several advantages that single sources don't. They can be used to increase the coverage angle without artifacts if the acoustic centers remain close and they can be used to achieve a narrow directivity pattern by proper selection of the array dimensions, source size and number of elements. Indeed, a valuable addition to our design tools.

9.5   The Effect of Wavefront Curvature on Line Arrays

There is a great deal of interest in the effect that the wavefront curvature of an individual element has on a line array's polar response. We know that for a line array, the curvature in the horizontal plane determines the horizontal coverage, but in the vertical plane the curvature of each element creates a scalloped source and we want to know how the elements interact to create the vertical polar response. We are interested in this problem because it is not really possible to get a flat wavefront from a finite source. With the tools that we have developed, we can easily calculate the effect that a vertical curvature of each element in a line array has on the array response.

Using Eq. (3.6.64) on page 62, where we will need to calculate the vertical DF, $F(kb \sin \phi)$ for our specific situation. This is easily performed by first calculating the DF for a single source and then multiplying by the DF for a vertical array of point sources (convolving the wavefront velocities with point sources)

$$F(kb \sin \phi) = \frac{\sin\left(n\, \dfrac{kb}{2}\sin\phi\right)}{n \sin\left(\dfrac{kb}{2}\sin\phi\right)} \times \int_{-b}^{b} v(z) e^{ik\, z \sin \phi}\, dz \qquad (9.5.11)$$

where $v(z)$ is the vertical velocity distribution in the cylindrical aperture

$$v(z) = \frac{l^2 e^{ik\left(\sqrt{z^2+l^2}-l\right)}}{l^2 + z^2} \qquad (9.5.12)$$

which we obtained from Eq. (4.2.13) on page 76. The first term in the Eq. (9.5.11) is for the line array of point sources and the second is for a curved source.

Fig. 9-11 shows the polar map for a line array of eight elements of height $2b$ with element spacing $2b$ and no curvature of the wavefronts in the vertical direction (top). In this case the second term above would be identical to Eq. (9.4.8). The angular range is limited to 30° because of the extreme directivity of the array in the vertical direction. The lower polar map is for the same array but with a vertical curvature of each element, which corresponds to a virtual wavefront radius $l = 2b$. This can be seen from Fig. 4-5 to be a substantial curvature. With the exception of the extreme off-axis results these two maps appear identical. There does not seem to be a substantial effect of element curvature, which is in stark contrast to both intuition and popular belief.
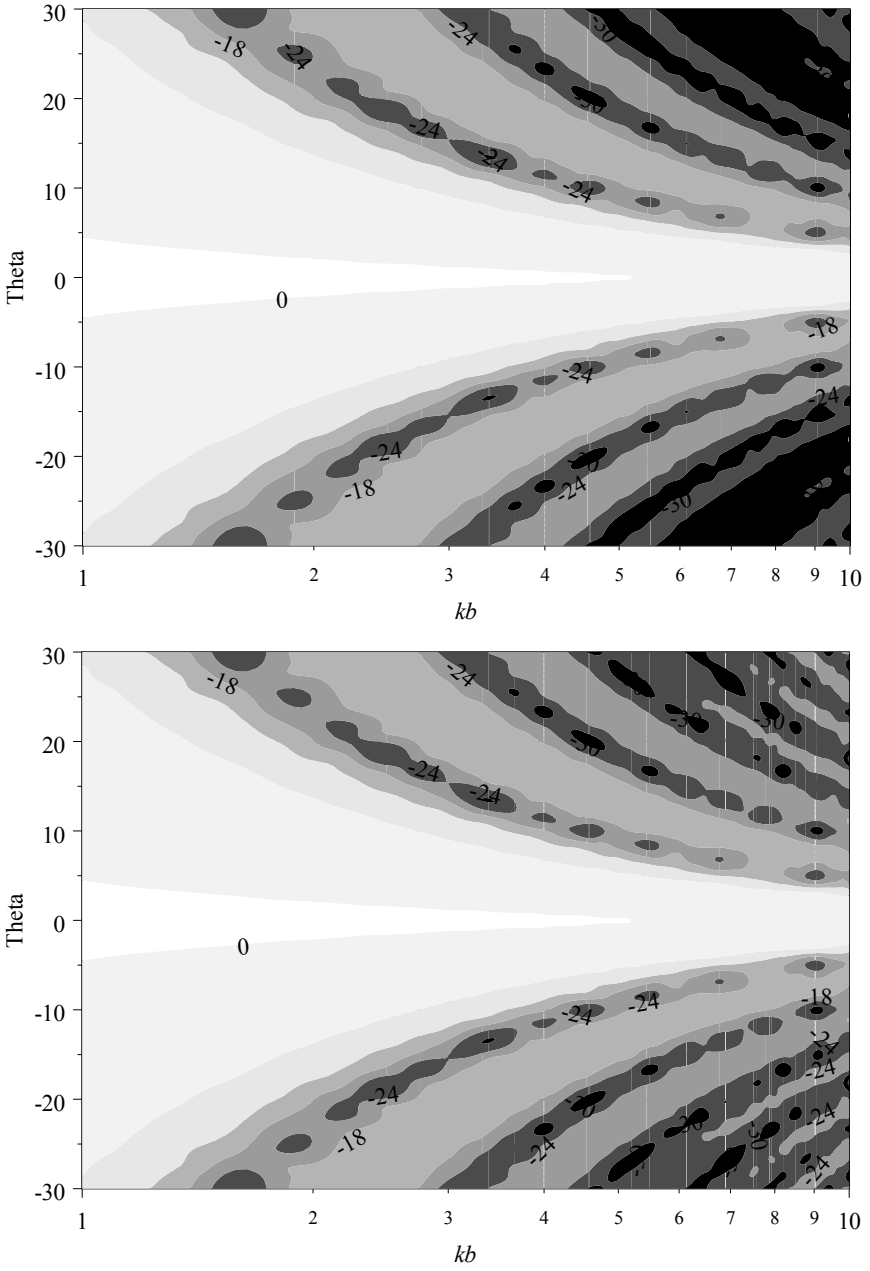
Figure 9-11 - 7 Element line array with no curvature (top) and a curvature of .5 b

It is easy to understand these results, however. In a line array the vertical response is dominated by the vertical extent of the array. We also saw this in the previous section. The details of the velocity distribution of an individual element simply does not enter into the problem. Mathematically this is to say that in Eq. (9.5.11) the result is dominated by the first term, which is far more strongly dependent on ϕ than the second term.

9.6   Cardiod Enclosures

This section may well have belonged in the chapter on enclosures, but it does involve multiple transducers used for directivity control and as such is also a good fit here. We have seen that placing more than one source in an enclosure generates a complex set of interactions mostly depending on the distance between the sources. We have looked primarily at arrays placed in a single plane. In this section, we will develop techniques for use in finite sized enclosures. These enclosures will be spheres, but the ideas can easily be extended to normal rectangular enclosures.

As we saw in previous sections one can place a source in a sphere and combine multiple sources by rotating them (and translating to a limited degree) and adding the far field responses. Consider the following example of what we may want to achieve.

The goal is to design an enclosure which has two transducers and which exhibits a cardiod directional pattern. (For more information on cardiod patterns, see Chap. 11). For our purposes it will be sufficient to require $p(\theta = \pi) = 0$.

Lets assume that one source is on the front of the sphere and the other on the rear. By summing these two sources weighted by a complex number, we can force this sum to obey the above equation. This procedure leads to

$$p(\theta, f) = p_f(\theta, f) + B(f) p_r(\theta - \pi, f) \tag{9.6.13}$$

p_f(theta,f) = the polar pattern for the front source

p_r(theta,f) = the polar pattern for the rear source

We have considered only one weighting factor since one is sufficient for directivity control. To control both the directivity and frequency response, we would have to use two complex coefficients.

By setting Eq. (9.6.13) equal to zero at $\theta = 0$ we can develop the function $B(f)$ as

$$B(f) = \frac{-p_f(\pi, f)}{p_r(0, f)} \tag{9.6.14}$$

Fig. 9-12 shows the polar map for the two source system with the rear source passed through the filter $B(f)$. This figure is shown as a function of ka, where a is the radius of the sphere. Fig. 9-13 shows the magnitude and phase of the complex filter $B(f)$ (solid) along with a first order low pass filter, shown as the dashed line. (Both filters are plotted as functions of ka.) Note that the magnitude of the sim-
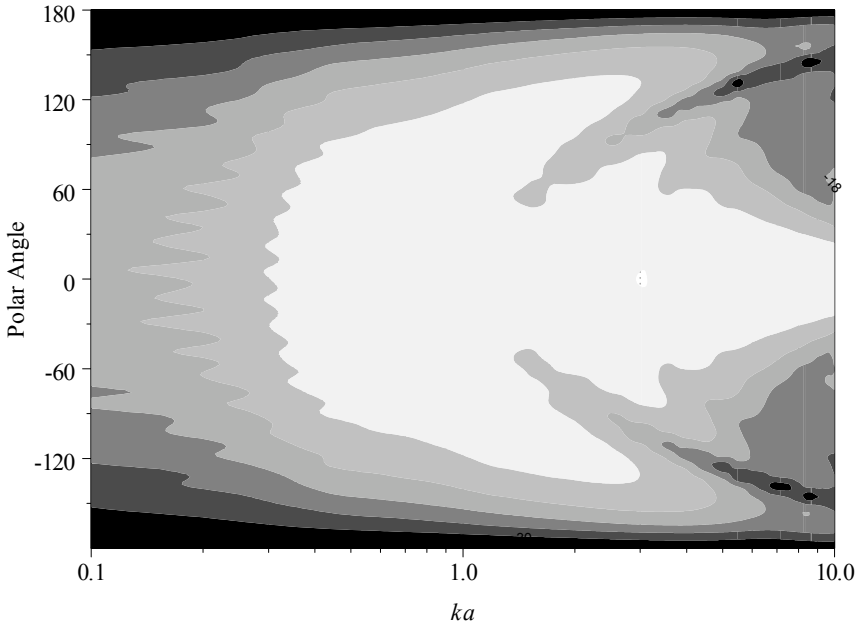
Figure 9-12 - Polar map of an electronically created cardiod pattern

ple filter is nearly correct, but the phase is wrong. Fig. 9-14 shows the polar map which would be obtained by the use of the simpler filter. It is not as good, but it does improve on a simple monopole.

The situation could be further improved with the use of delay in the filter, which is in line with the rearward facing source. This would give a better match to the phase response of the desired filter. Delay is not trivial to obtain, but it can be achieved with either passive or active means. (With DSP, it is trivial.) The design of this all-pass filter is not something that we will be covering here.

It is also possible with the above technique to obtain a whole array of polar responses. Each of these responses has a particular polar pattern, which will come with a particular axial response – the two results are linked. Fig. 9-15 shows the axial responses for the various configurations. The Hyper-cardiod has a null forced at $3\pi/4$ and the bipole has one forced at $\pi/2$. (Note: These responses are in addition to the response of the sources themselves.)

Finally, it should be obvious that directivity functions of even higher orders can be obtained in exactly this same manner with the addition of more sources. Each additional source yields an additional degree of freedom and a potentially higher order directivity function.
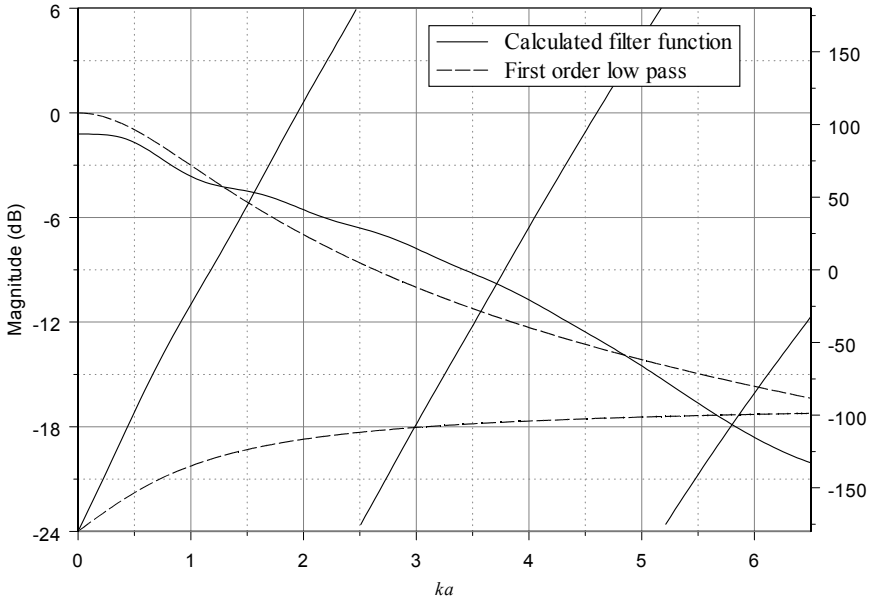
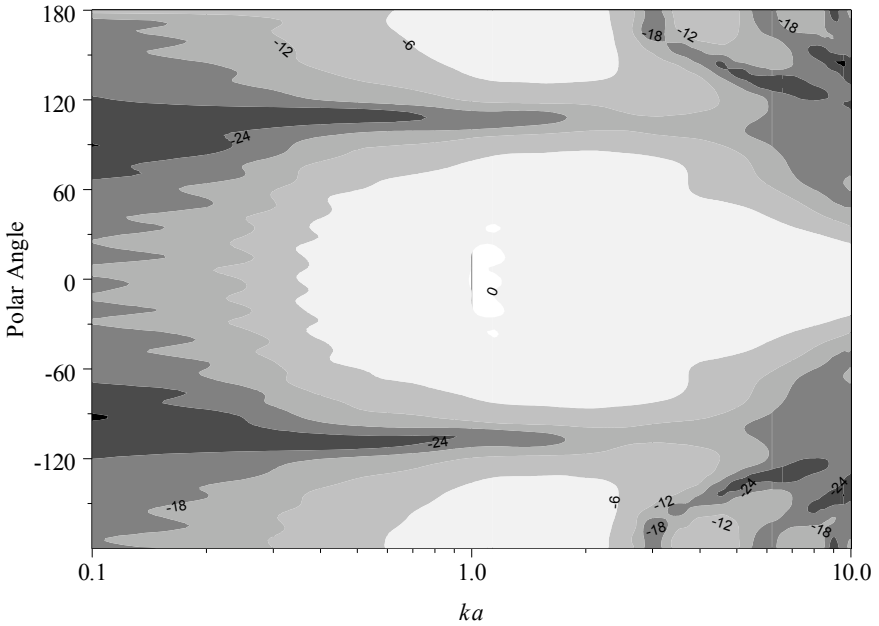*Figure 9-13 - Magnitude and phase of cardiod filter*

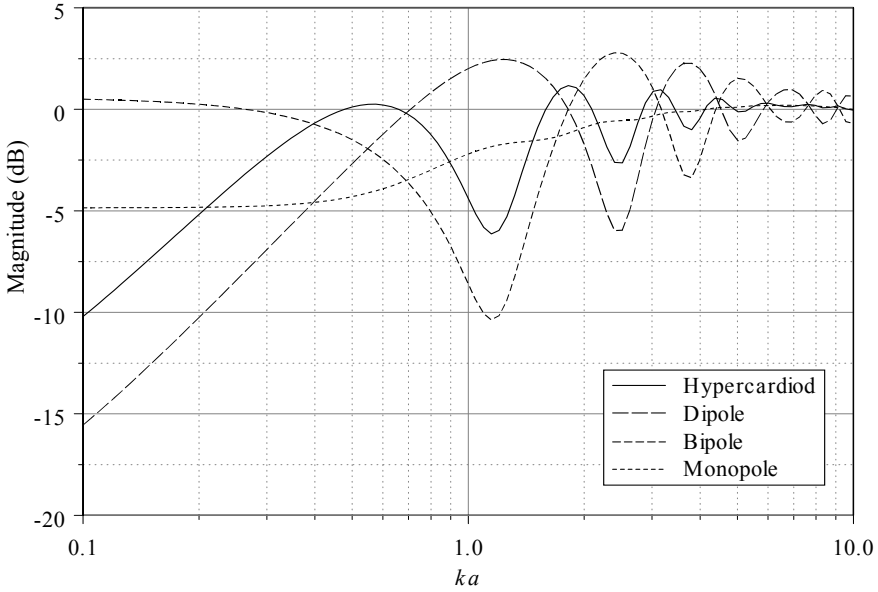*Figure 9-14 - Polar map for a cardiod array with a simple 1st order filter*

Figure 9-15 - Axial frequency response for higher order enclosure

9.7   Passive Low Frequency Directivity

Perhaps the best known way to obtain low frequency directivity is with the use of a dipole. A dipole yields a stable polar pattern over a large bandwidth, but suffers from poor efficiency. The question naturally arises as to the possibility of obtaining a more directional response at low frequencies without the poor performance in output. Another thing that makes this problem interesting is that it will use many of the tools that we have assembled in this text. We will combine the T-matrix calculation with a spherical polar model in order to investigate the possibility of obtaining the response that we seek.

Rather than go down what turns out to be a dead end, we will simply state that there is no possibility of any real degree of directivity control for closed, ducted port or passive radiator ported enclosures. There just is nothing that one can do with these type of enclosures.

Consider the following system as shown in Fig. 9-16. This system uses a lever in the reverse form from how it is normally used. The idea is that by tuning the lever very high in frequency, above the passband, that its output will "track" that of the source, but with a diminished amplitude thus giving a combination of a monopole and a dipole response. We hope that this combination will have greater efficiency than a dipole but with a narrower directivity than a monopole. We will analyze this configuration in order to ascertain how close we can come to our objective.
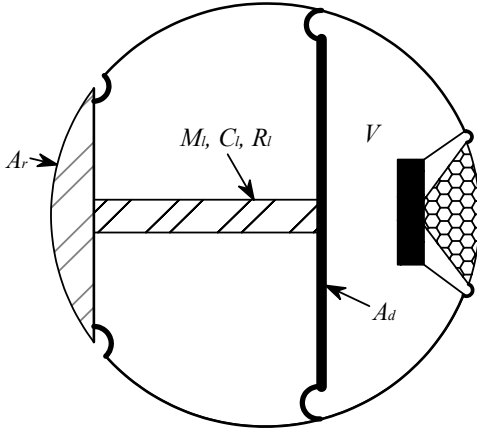
M_l, C_l, R_l

V

A_r

A_d

Figure 9-16 - Example enclosure for cardiod system

We start by using the T-matrix equations for an Acoustic Lever™ from which we can derive the following results

$$z_d(\omega) = \frac{-iS_d^2\left(M_l\omega^2 - i\omega R_l - 1\right)\rho c^2}{\omega\left(\dfrac{V}{C_l} + A_d^2\rho c^2 - VM_l\omega^2\right)}$$

(9.7.15)

$$V_d(\omega) = \frac{S_d Bl_d}{Re_d z_d(\omega) + Re_d\left(-i\omega M_d + R_d + \dfrac{1}{-i\omega C_d}\right) + Bl_d^2}$$

(9.7.16)

$$T(\omega) = \frac{1}{-i\omega\,\dfrac{V}{\rho c^2}\,\dfrac{-i\omega M_l + \dfrac{1}{-i\omega C_l} + R_l}{A_r A_d} + \dfrac{A_d}{A_r}}$$

(9.7.17)

$z_d(\omega) =$ *the acoustic load on the rear of the diaphragm*

$V_d(\omega) =$ *the transfer function from the input voltage to the diaphragm velocity*

$T(\omega) =$ *the transfer function from the diaphragm velocity to the lever velocity*

$M_l =$ *the lever mass*

$C_l =$ *the lever compliance*

$R_l =$ *the lever resistance*

$A_d =$ *lever driven area*

$A_r =$ *lever radiating area*

$V =$ *volume between lever and source*

$X_d =$ *driver parameters*

From this set of equations, we can calculate the velocities of both the source and the lever.

We will also need the equation for the radiated pressure from a sphere

$$p(ka,\theta) \propto \sum_{n=0}^{20} A_n P_n(\cos\theta) \frac{h_n\left(ka\frac{r}{a}\right)}{h_n'(ka)} \tag{9.7.18}$$

$a = radius\ of\ the\ sphere$
$r = the\ field\ radius >> a$

where we have left off constants since we will only be dealing with relative values here. The A_n's are the values for a rigid spherical cap (Sec. 3.5 on page 51)

We can now write our answer as (in the variable ka)

$$p(ka,\theta) = V_d\left(ka\frac{c}{a}\right)\left(p(ka,\theta) + T(ka\frac{c}{a})p(ka,\theta-\pi)\right) \tag{9.7.19}$$

The example that we will show here has a typical loudspeaker in an average sized woofer enclosure one meter in diameter. The lever is light and stiff with a lot of damping. There are so many degrees of freedom in the lever design that the specific numbers would not mean much. What we will show here is a simple example of a monopole, a dipole and the cardiod system with a rear lever all normalized to the monopoles high frequency response (which would be nearly the same for all of these systems).

When these calculations are made, the resulting system is seen to rise slightly with frequency – just as the dipole does, but greater than a monopole. A simple first order LP filter in series with the dipole and cardiod systems would "flatten" the response. The cardiod would require another higher order LP filter to suppress the large resonance of the lever. The axial responses for all three of these systems are shown in Fig. 9-17.

At the lowest frequencies, the cardiod has the greatest extension and the greatest output. With rising frequency, the monopole quickly gains in output, followed by the dipole. The cardiod tracks the dipole with only a few dB less output in the mid-band. The monopole and dipole both have omni-directional response throughout the bandwidth shown. The polar map for the Acoustic Lever™ cardiod enclosure is shown in Fig. 9-18. The cardiod has a better directivity than the monopole, but without the low frequency loss of the dipole. Each of these systems has advantages and disadvantages.

9.8   Summary

Arrays – multiple sources covering a common bandwidth – offer an added flexibility in controlling the directional patterns of what are otherwise uncontrollable single source patterns. By using these techniques one has a much greater design flexibility and can achieve a constant narrow directivity to a much lower frequency than what is practical with the waveguide approach.
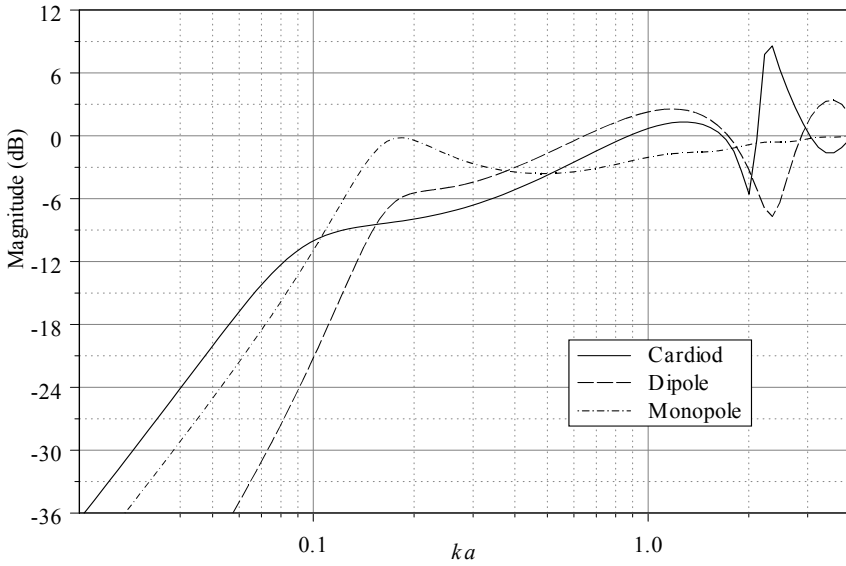
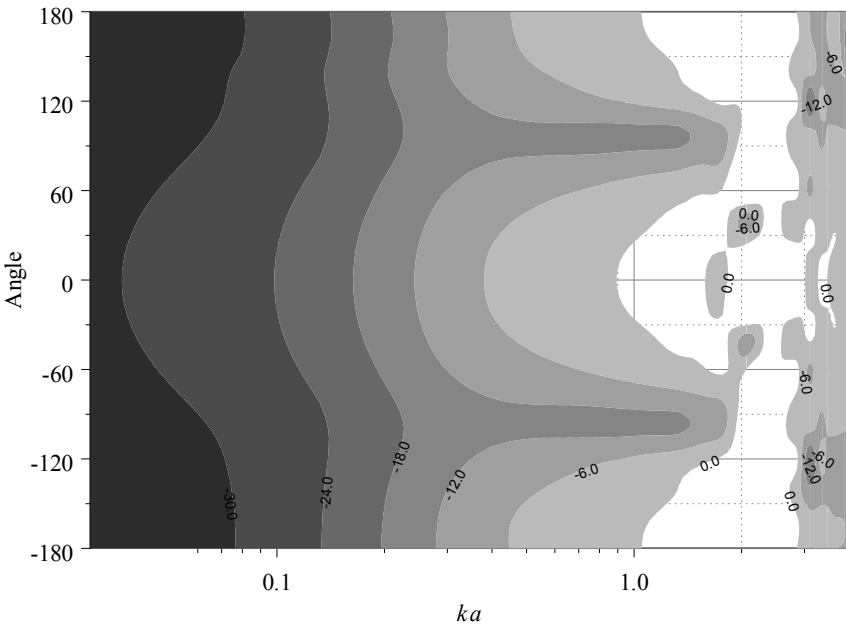*Figure 9-17 - Axial response for monopole, dipole and cardiod*

Figure 9-18 - Polar map for Acoustic Lever™ cardiod enclosure